Journal of Geochemical Exploration 161 (2016) 16–26

Contents lists available at ScienceDirect

Journal of Geochemical Exploration

journal homepage: www.elsevier.com/locate/jgeoexp

Multilevel hydrogeochemical monitoring of spatial distribution of arsenic: A case study at Datong Basin, northern China

Kunfu Pi, Yanxin Wang *, Xianjun Xie, Yaqing Liu, Teng Ma, Chunli Su

State Key Laboratory of Biogeology and Environmental Geology & School of Environmental Studies, China University of Geosciences, 430074 Wuhan, China

ARTICLE INFO

Article history:
Received 12 September 2014
Revised 9 August 2015
Accepted 6 September 2015
Available online 11 September 2015

Keywords:
Arsenic mobilization
Redox processes
Hydrochemical monitoring
Groundwater

ABSTRACT

To elaborate primary geochemical factors controlling the enrichment and spatial distribution of arsenic (As) species in groundwater systems, multilevel hydrogeochemical monitoring was conducted at an As-contaminated site in central part of Datong Basin, northern China. Aqueous As concentration was highly variable, ranging from 5.47 to 2690 μg/L. High As groundwater was characterized by elevated HCO_3^-, Fe(II), HS^-, NH_4^+ and dominated by As(III) species. The positive correlation between As and Fe contents was observed in easily-reducible Fe pool, indicating that poorly crystalline Fe minerals served as an important As sink via chemical adsorption and/or co-precipitation. Under moderately reducing and weakly alkaline conditions (Eh ≥ 100 mV and pH between 7.69 and 8.04), As mobilization could be controlled by pH-dependent desorption process. The relationships of aqueous As(V) and As(III) versus Fe(II) concentration confirm that reductive dissolution of As-bearing Fe oxides/hydroxides and reductive desorption of As(V) could be responsible for As enrichment and As(III) predominance in groundwater under more reducing conditions (Eh ≤ 100 mV). The co-presence of elevated As(III) and sulfide indicates that microbial sulfate reduction may promote As(V) transformation into thioarsenate and/or thioarsenite and further into As(III). However, the correlations of As(V) and As(III) concentration versus saturation indices of mackinawite suggest that decrease in aqueous As concentration may be due to re-sequestration of both As(V) and As(III) by Fe(II)-sulfide precipitates.

1. Introduction

Geogenic arsenic (As) contamination of groundwater has attracted worldwide concern due to the severe health damage of waterborne chronic arsenic poisoning, especially in India, Bangladesh, Cambodia, Vietnam and China (Eiche et al., 2008; Polizzotto et al., 2005; Polya et al., 2005; Wang et al., 2009). At Datong Basin, one of the most water-scarce regions in northern China, naturally occurring high As (>10 μg/L) groundwater has posed a serious threat to the health of a large population that relies on groundwater as a main resource for drinking and agriculture purposes (Guo et al., 2003; Wang et al., 2009). Diverse symptoms of severe arsenic poisoning (e.g., hyperpigmentation, hyperkeratosis, peripheral neuropathy, skin, liver and bladder cancers) resulting from long-term intake of high As groundwater arose in lots of inhabitants, particularly those residing in central areas of the basin. Given the importance of groundwater as a vital resource for sustainable water supply, it is imperative to comprehend hydrogeochemical processes responsible for As mobilization and develop suitable technology to rehabilitate As-contaminated aquifers.

Reactive transport of As depends on its chemical speciation and pH condition. Generally, groundwater As mainly occurs in inorganic forms of arsenate (As(V)) and arsenite (As(III)) (Smedley and Kinniburgh, 2002). Under circum-neutral to alkaline conditions, As(V) primarily exists as $H_2AsO_4^-$ or $HAsO_4^{2-}$ ($pK_2 = 6.97$ for H_3AsO_4) and As(III) as H_3AsO_3 ($pK_1 = 9.23$ for H_3AsO_3). Negatively charged As(V) binds strongly to the surfaces of Fe oxides/hydroxides and hence is greatly retarded via chemical adsorption (Dixit and Hering, 2003; Giménez et al., 2007). However, As(V) adsorption is greatly affected by pH condition and can be largely mobilized with the increase in pH value (especially over 8.5) (Dixit and Hering, 2003; Smedley and Kinniburgh, 2002). Besides, As(V) adsorbed on substrate surfaces can be migrated by other competing anions in groundwater, such as PO_4^{3-}, HCO_3^- and SO_4^{2-} (Kanematsu et al., 2013; Radu et al., 2005; Zhao and Stanforth, 2001). In contrast, neutral H_3AsO_3 is much weakly adsorbed on Fe oxides/hydroxides, and its adsorption little depends on pH value and the competing anions under similar conditions. Both As(V) and As(III) species can be adsorbed to other substrates, including clay minerals, calcite and mackinawite, which makes the sorption/desorption reactions of As species more complicated (Manning and Goldberg, 1997; Roman-Ross et al., 2006).

Redox potential (Eh value) is another key factor influencing As speciation and its mobilization. Under oxidizing conditions, As(V) species is normally dominant, while the As(III) species predominates in As speciation under reducing conditions (Smedley and Kinniburgh, 2002). It was documented that many high As aquifers around the world were

* Corresponding author.
E-mail address: yx.wang@cug.edu.cn (Y. Wang).

http://dx.doi.org/10.1016/j.gexplo.2015.09.002
0375-6742/

mildly to strongly reducing and a large amount of aqueous As existed as the reduced As(III) species (Charlet et al., 2007; Fendorf et al., 2010; Postma et al., 2007). Since As(III) species is more toxic and mobile than As(V), it is important to understand the transformation between them and geochemical processes regulating As(III) transport in aquifers. Several redox reactions are closely associated with the transformation and transport of As species (Postma et al., 2007). For instance, both abiotic reduction of As(V) by sulfide or reducing organic carbon and biotic reduction through accepting electrons from the biodegradation of natural organic matter (NOM) or microbial oxidation of sulfide have been identified in the transformation As speciation (Burton et al., 2011; Fisher et al., 2008; Jiang et al., 2009). Subsequent desorption of As(III) can facilitate remarkable accumulation of As in groundwater (Burton et al., 2013). Under appropriate reducing conditions, direct As(V) reduction accompanying with Fe(III) reduction leads to As release from the surfaces of Fe minerals or formation of weakly adsorbed complexes that are readily re-mobilized (Bose and Sharma, 2002). On the other hand, microbially mediated reduction of sulfate to sulfide can promote the formation of thioarsenic and iron sulfide minerals (Fisher et al., 2008; Kirk et al., 2004). The retention of As in sulfate-reducing environment is thus highly related with the formation of Fe(II) sulfide minerals, such as mackinawite, pyrite and arsenopyrite that are able to incorporate As to different extents, depending on the redox state of As species (Bostick et al., 2004; Pedersen et al., 2006).

High As concentration over 1 mg/L in groundwater has been widely detected at Datong Basin, especially in the central-south part of the basin (Xie et al., 2008). Geochemical behaviors of As in groundwater systems were recognized to relate with (bio)geochemical cycling of Fe oxides/hydroxides, sulfate and organic carbon that could be catalyzed by microbial activities (Xie et al., 2013b). As mobilization in shallow aquifers was linked to desorption processes of As from Fe mineral surfaces and reductive dissolution of As-bound Fe oxides/hydroxides (Xie et al., 2008; Xie et al., 2009). Other relevant processes, such as the presence of NOM, transformation between different Fe minerals and formation of As-bearing secondary minerals, also were considered to exert influences on As transport (Xie et al., 2013a). However, in order to better evaluate the transport of As in the groundwater systems, it is necessary to understand the distribution and transformation of As speciation as well as to which solid phases different As species are bound to during transport processes.

Therefore, in this study, hydrogeochemical investigation at a multilevel field monitoring site and subsequent laboratory experiments were conducted to identify the principal factors. Specific objectives include: (1) to characterize spatial distribution of As species in groundwater and in aquifer sediments, (2) to examine hydrogeochemical conditions governing different extents of As(III) and As(V) enrichment in groundwater, and (3) to elaborate redox transformation and geochemical processes regulating the mobilization of As(III) and As(V) species. The results provide not only new insights into environmental behaviors of As in groundwater systems, but also important information for water resource management in Datong Basin.

2. Site description

Datong Basin is a typical Cenozoic basin, one of the most water-scare regions in northern China (see Wang et al. (2009) for a detailed description). High As groundwater mainly occurs in shallow semi-confined Quaternary aquifers consisting of late Pleistocene and Holocene unconsolidated alluvial-lacustrine sediments within the depth of 10 to 50 m below the land surface. Groundwater flow is sluggish with a velocity of approximate 0.2 to 0.5 m/d, and groundwater table is less than 3 m in the central area. Groundwater As concentration generally increases with depth less than 50 m and then decreases with depth over 50 m below the land surface (Xie et al., 2008). Groundwater with highest As concentration occurs in aquifers at depths between 15 and 40 m and has been extracted by local residents for domestic and irrigation use.

To reveal the distribution patterns of groundwater As and its speciation, we constructed a multi-level monitoring network at a site located in the central area of Datong Basin based on our preliminary hydrogeological and geophysical survey (DY Site, Fig. 1a). Within the 150×250 m^2 site, there was a gentle hydraulic gradient roughly sloping from SW toward the NE, further reaching the Sanggan River as a potential discharge zone (Fig. 1b). The shallow aquifers at depth less than 50 m below the land surface were selected because of high As concentration in groundwater. There were three relatively independent semi-confined aquifers at depths of 19 m, 26 m and 38 m respectively below the land surface (Fig. 1c). Clay and silty clay interlayers functioned as aquitards to prevent the infiltration of atmospheric oxygen and maintain the anoxic environment of underlying aquifers. Sediment materials of the three aquifers were fine to medium sands or sandy silts with gray, dark gray or black color that mainly consisted of Fe mineral-coated quartz particles, feldspar, carbonates, illite and chlorite. The site was instrumented with a series of 32 multilevel wells screening the three aquifers for hydrochemical monitoring and groundwater sampling (Fig. 1b).

3. Materials and methods

3.1. Sampling

A total of 32 groundwater samples from the multilevel monitoring wells were collected in August, 2013. For each multilevel monitoring site, capital letters are added to its ID number to distinguish its location at the Shallow (S), Middle (M) and Deep (D) aquifer, respectively. After pumping for at least 10 min, groundwater samples were collected using a peristaltic pump. Temperature (T), pH, electrical conductivity (EC) and Eh values were measured on site using an YSI 600XLM portable meter calibrated before use. Samples for determination of Fe(II), HS^-, NH_4^+ using the spectrophotometry (HACH, DR2800) and alkalinity with the Gran titration method were taken and measured immediately in the field laboratory. These samples were collected with a syringe and directly filtered (<0.45 μm) into prepared colorimetric reagent solutions. Samples for laboratory measurement of anions and cations were filtered (<0.45 μm) using a vacuum pump and collected into two acid washed and pre-cleansed 50 mL HDPE bottles. Those for cation analysis were acidified with ultra-pure HNO_3 to pH < 2, whereas the anion samples were not treated. Samples for As analysis were filtered, species separated with LC-SAX anion-exchange resin (Sigma-Aldrich) in the field laboratory (Le et al., 2000; Sugár et al., 2013), and acidified to pH < 2 with ultra-pure HCl. After activation, the anion-exchange resin could retain As(V) but not As(III). Thus As(V) concentration was obtained by calculating the difference between total As and As(III), assuming that organic As was negligible.

Samples for DOC analysis were also filtered, acidified to pH < 2 with ultra-pure HCl, and stored in 50 mL special amber glass bottles wrapped up with aluminum foil and sealed by designed caps to prevent light and air exposure. After collection, all samples were stored in 4 °C refrigerator. Laboratory determination was conducted with one week after sampling.

At the same time, ten boreholes were drilled to collect sediment samples from these aquifers where the monitoring wells were installed. Sediments were retrieved from depths of 0 to 40 m below the land surface and core samples were collected at the corresponding depths. After collection, the core samples were immediately capped into PVC casings, sealed to eliminate air exposure, and stored at 4 °C in the dark. Sediment analysis was performed within two weeks after sampling.

3.2. Analytical methods

3.2.1. Hydrochemical analysis

Major cations constituents of water samples were analyzed by inductively coupled plasma optical omission spectrometry (ICP-OES)

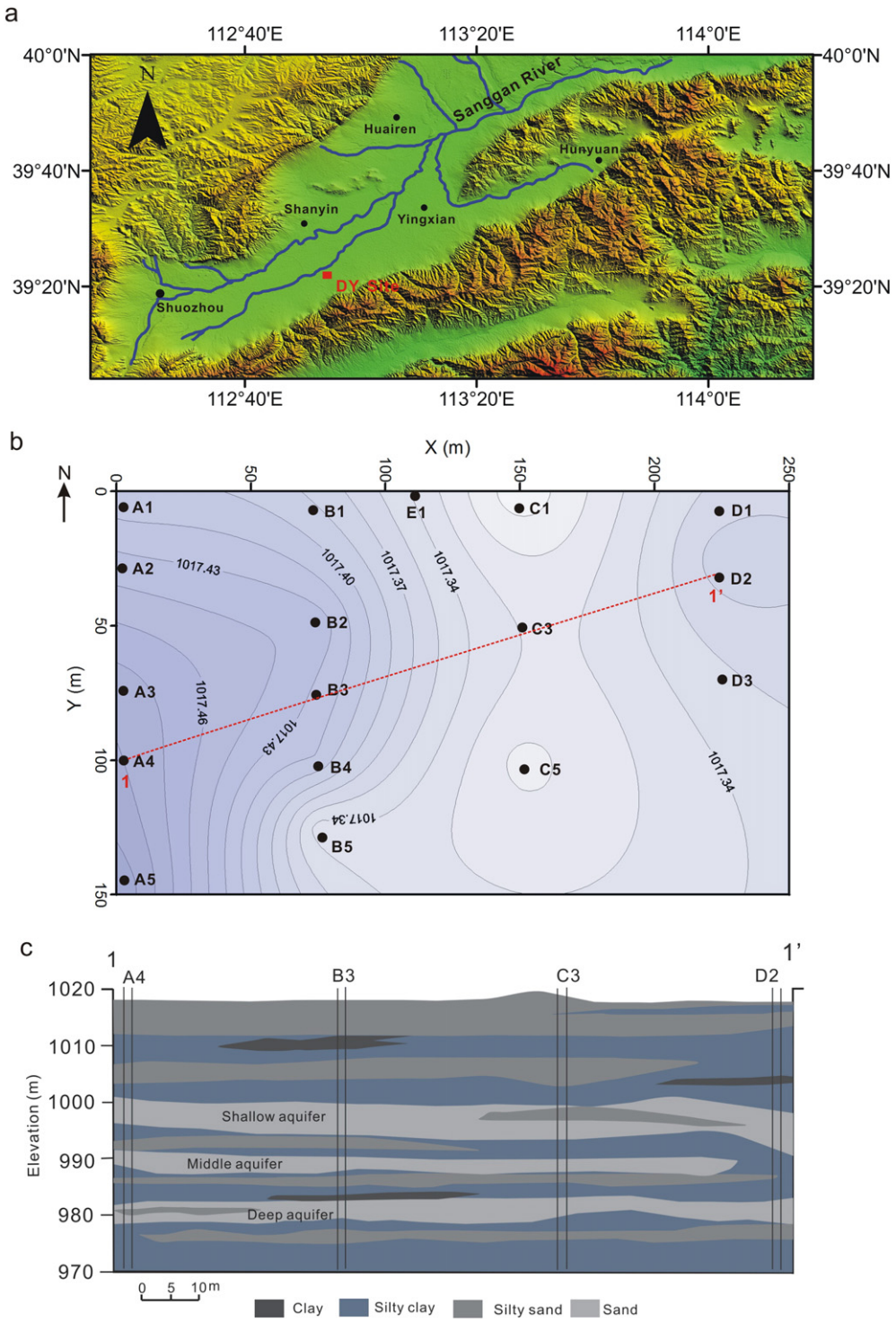

Fig. 1. (a) Location of the field monitoring site (DY Site); (b) Plan view of the study site and monitoring wells, the labeled solid circles denoting the monitoring wells and the lines with numbers the groundwater table contours; (c) Hydrogeological cross section along the 1–1′ line in (b), with the Shallow (S), Middle (M) and Deep (D) aquifer marked.

(ICAP6300, Thermo Scientific) and trace constituents by inductively coupled plasma mass spectrometry (ICP-MS) (Perkin Elmer ELAN DRC-e). Anion concentration of water samples was measured using ion chromatography (IC) (Metrohm 761 Compact IC). Total As and As species separated in the field were determined by hydride generation atomic fluorescence spectrometry (HG-AFS) (AFS-820, Titan). Dissolved organic carbon (DOC) concentration was determined on the acidified samples using the high-temperature catalytic combustion method with the TOC analyzer (TOC-V, Shimadzu), generating data with a standard deviation of ±2%. For every eight samples, both (mixed) standards prepared from the primary standard solutions (Sigma-Aldrich, Supelco) with 18.25 MΩ-cm deionized water and sample replicates were tested as an analysis routine for cations, anions and As determination. Unless otherwise stated, the analytical reproducibility was generally within 5% relative to all components analyzed. Field and laboratory blanks were below the detection limits for all the components.

Calculations of ion activities and saturation indices (SI) of mackinawite (FeS_m) were performed using the public domain code PHREEQC version 2.18 with the thermodynamic values from the

PHREEQC database. The Eh-pH diagram for As–Fe–S system containing 2×10^{-5} M total As, 1×10^{-4} M total Fe and 1×10^{-4} M total S was generated using the software HSC Chemistry 7.0 at 25 °C and under 1 bar. Groundwater samples were plotted on the diagram to model As species and related compositions. Stability fields of $\equiv OHAsO_4^{3-}$ ($HAsO_4^{2-}$ sorption complex on hydrous ferric oxides (HFO)), thioarsenic (Thio-As) and Fe(II) sulfides (FeS_x) including mackinawite (FeS_m) and pyrite (FeS_2) were also referred to the results of Omoregie et al. (2013).

3.2.2. Sediment analysis

Aliquots of sediment samples from different boreholes were analyzed for total As and Fe contents, and sequentially extracted to distinguish pools of solid-phase As and Fe species. Fresh sediment samples were air-dried and ground, and 0.05 g subsample was digested with 2 mL ultra-pure concentrated HNO_3, 0.5 mL 30% H_2O_2 and 1 mL concentrated HF at 180 °C for 24 h, evaporated to near dryness and diluted to 100 mL with 2% (V/V) HNO_3 prior to determining concentration of total As and Fe by HG-AFS and ICP-OES, respectively. The average errors calculated with the methods referred to above for As and Fe determination were both within 5%.

Subsamples for sequential extraction were obtained from the center of the cores to avoid the effect of possible oxidation and immediately freeze-dried after sampling. Sequential extraction was performed following procedures below to target specific solid-phases to which As may be bound, without changes in As redox speciation (Höhn et al., 2006; Keon et al., 2001):

(1) Weakly adsorbed: 1 M $MgCl_2$, 2 h;
(2) Strongly adsorbed: 1 M NaH_2PO_4, pH = 5, 24 h;
(3) Easily reducible Fe phase bound: 1 M hydroxylamine hydrochloride, 24 h;
(4) Crystalline Fe phase bound: 1 M HCl, 24 h.

0.2 g fresh subsample was added to a 50 mL HDPE centrifuge tube, mixed with 20 mL extraction solution under N_2 atmosphere, and extracted for the set time in an overhead shaker. In every step, the extractant was centrifuged at 5000 rpm for 20 min, decanted from the tubes, filtered (<0.45 μm), and analyzed for As and Fe species. The determination of As species by HG-AFS was conducted with following procedures (Höhn et al., 2006): the concentration of As(III) species in diluted extractant was first determined using optimized hydride generation conditions by the combination of HCl (2%–3%, V/V) and KBH_4 (2 wt.% in 0.5 wt.% KOH) to reduce As(III) solely; total As concentration in subsamples was then measured after treatment by ascorbic acid-KI solution (0.4 L HCl, 20 g ascorbic acid and 20 g KI diluted to 1 L), generating an analytical precision of ±10%. The Fe(II) concentration in diluted extractant was measured using the spectrophotometer (HACH, DR2800) after adding prepared Ferrozine reagent to a 10 mL aliquot of the sample. Total Fe content was analyzed using Ferrozine reagent after being reduced by 10 wt.% hydroxylamine hydrochloride. The analytical error for Fe(II) and Fe determination using Ferrozine method was better than 5%.

4. Results and discussion

4.1. Hydrochemistry

The hydrochemical characteristics and groundwater constituents are summarized in Table 1, and the major chemical compositions are plotted on the Piper diagrams in Fig. 2. The pH values of groundwater samples varied from 7.69 to 8.34 with an average of 8.09, indicating near-neutral to weakly alkaline conditions. The groundwater had Na–HCO_3 and Na–HCO_3–SO_4–Cl types both in the Shallow and Middle aquifers and Na–HCO_3 type in the Deep aquifer (Fig. 2). Major anions

Table 1
Summary of physico-chemical parameters and chemical constituents of groundwater samples.

	Max.	Min.	Aver.	S.D.
T (°C)	9.15	8.20	8.75	0.23
pH	8.34	7.69	8.09	0.14
Eh (mV)	−31.9	−221.7	−140.4	44.5
Ca (mg/L)	30.98	4.40	13.81	5.51
Mg (mg/L)	39.05	8.93	21.79	6.94
Na (mg/L)	440.3	62.75	144.3	89.75
K (mg/L)	1.58	0.15	0.61	0.28
HCO_3^- (mg/L)	663	268	399	88
SO_4^{2-} (mg/L)	349	4.15	48.8	83.8
Cl^- (mg/L)	222	17.9	54.7	66.8
F^- (mg/L)	2.54	0.33	1.12	0.62
Br^- (μg/L)	338	61.5	122	85.2
Fe(II) (mg/L)	0.24	0.01	0.08	0.06
Fe (mg/L)	0.27	0.04	0.12	0.06
HS^- (μg/L)	293	1	46	54
NH_4^+ (mg/L)	1.53	0.01	0.57	0.45
NO_3^- (mg/L)	0.13	n.d.	n.d.	n.d.
HPO_4^{2-} (mg/L)	0.13	n.d.	n.d.	n.d.
DOC (mg/L)	21.89	5.29	9.39	3.45
Mn (μg/L)	184	42.4	110	38.9
Al (μg/L)	103	1.90	7.71	17.5
As (μg/L)	2690	5.47	697	664
As(III) (μg/L)	2310	0.03	528	524

Notes: n.d.: not detected; NO_3^- only detected in well A1 (0.13 mg/L) and E1 (0.06 mg/L) of the Shallow aquifer; HPO_4^{2-} only detected in well A1 (0.13 mg/L) of the Shallow aquifer.

in groundwater from the three aquifers are dominated by HCO_3^-, ranging from 268 to 663 mg/L with a mean value of 399 mg/L. Apart from few samples from the Shallow and Middle aquifers, the concentration of Cl^- and SO_4^{2-} was generally low (av. 54.7 mg/L and 48.8 mg/L, respectively). The cations in groundwater were dominated by Na^+, varying from 62.75 to 440.3 mg/L with an average of 144.3 mg/L. The concentration of Ca^{2+} and Mg^{2+} was much lower, with a mean value of 13.81 and 21.79 mg/L, respectively. Elevated Na^+ may be attributed either to its partitioning into the aqueous phase out of secondary mineral phases or to its exchange with Mg^{2+} and Ca^{2+} on the surfaces of clay minerals (Wang et al., 2009). The concentration of NO_3^- and HPO_4^{2-} was below detection limits (0.01 mg/L) in most groundwater samples, while the concentration of dissolved Fe and Mn was high with a mean value of 0.12 mg/L and 110 μg/L, respectively (Table 1).

Groundwater Eh value ranging from −221.7 to −31.9 mV indicate that reducing conditions, compatible with the reduction of Fe(III) and sulfate, evolved in aquifers (Borch et al., 2010). Prevailing reducing conditions were further confirmed by high aqueous Fe(II) and HS^- concentration up to 0.24 mg/L and 293 μg/L, respectively (Table 1). Within the anoxic aquifers, microbially mediated reduction of NO_3^-, Fe(III), and SO_4^{2-} was coupled to organic carbon biodegradation to produce NH_4^+, Fe(II), sulfide and HCO_3^- respectively into groundwater (Freikowski et al., 2013), as evidenced by our previous study on C, S and Fe isotopes at Datong Basin (Xie et al., 2013b).

4.2. Arsenic in groundwater

Total dissolved As concentration in groundwater samples was highly variable, ranging from 5.47 to 2690 μg/L with an average of 697 μg/L; 29 out of 32 samples contained As higher than the WHO recommended limit value of 10 μg/L for drinking water (WHO, 2001), and 5 samples even exceeded 1000 μg/L. The spatial distribution of groundwater As in the Shallow aquifer (Fig. 3a) showed that As concentration generally increased from the upper boundary (A1–D1) to the central area around borehole No. C5. The highest As concentration was detected at borehole No. C5 with a value of 2630 μg/L, and low As concentration (<10 μg/L) at borehole No. A1, B1 and B2 (within the red line, Fig. 3a). The high variability of As concentration in groundwater was associated with that of hydrogeochemical conditions. For instance, high As groundwater from

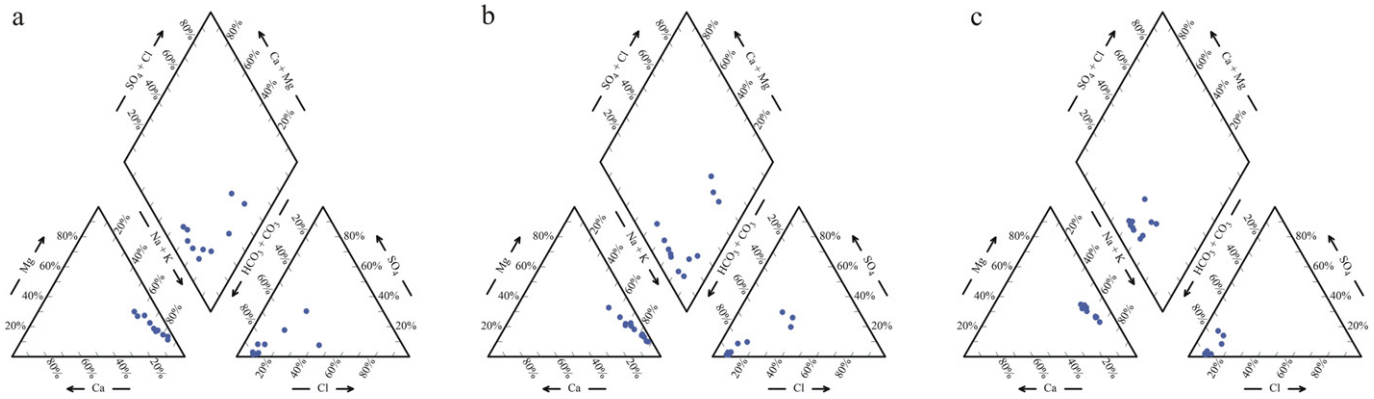

Fig. 2. Piper diagrams of groundwater samples from the (a) Shallow, (b) Middle, (c) Deep aquifer.

borehole No. C5 had lower Eh value, higher HS^- and Fe(II) concentration, while for groundwater from borehole No. A1, low As concentration was accompanied with higher Eh value and low concentration of HS^- and Fe(II). This clearly indicates that the spatial distribution of As in this area is significantly influenced by the redox conditions, with high As in groundwater generally occurring under reducing environment (Polya et al., 2005; Stüben et al., 2003; Xie et al., 2013a, 2013b). Similar to the Shallow aquifer, high variability of As concentration was observed in the Middle aquifer (Fig. 3b). Apart from borehole No. C5, groundwater sample from borehole No. A4 also contained fairly high As (1840 μg/L). The relatively low As zone was located along the line B1–B3 and around borehole No. A1, while As concentration less than 10 μg/L was almost undetectable (see Fig. 3b). The As distribution in the Deep aquifer appeared quite distinct (Fig. 3c), exhibiting a small variation relative to the Shallow and Middle aquifer, ranging from 411 to 763 μg/L with an average of 546 μg/L. Highest As concentration in this aquifer was detected around borehole No. B2 and C1 that had low As concentration in the Shallow and Middle aquifer.

Groundwater As(III) concentration varied from 0.03 to 2310 μg/L, averaging at 528 μg/L. As(III) was the dominant As species in groundwater, accounting for 0.4% to 87.9% (av. 67.9%) of total dissolved As. Spatial distribution patterns of As(III) resembled to those of total dissolved As (Fig. 3d–f), except little difference in the Deep aquifer that high As(III) zone occurred around borehole No. C1. The similar distribution patterns between As(III) and total As should be ascribed to the predominance of As(III) species.

Results of our previous studies indicated that As mobilization was mainly related to desorption of As from Fe mineral surfaces and reductive dissolution of Fe(III) oxides/hydroxides under alkaline and reducing conditions (Xie et al., 2008). In the study site, elevated As concentration

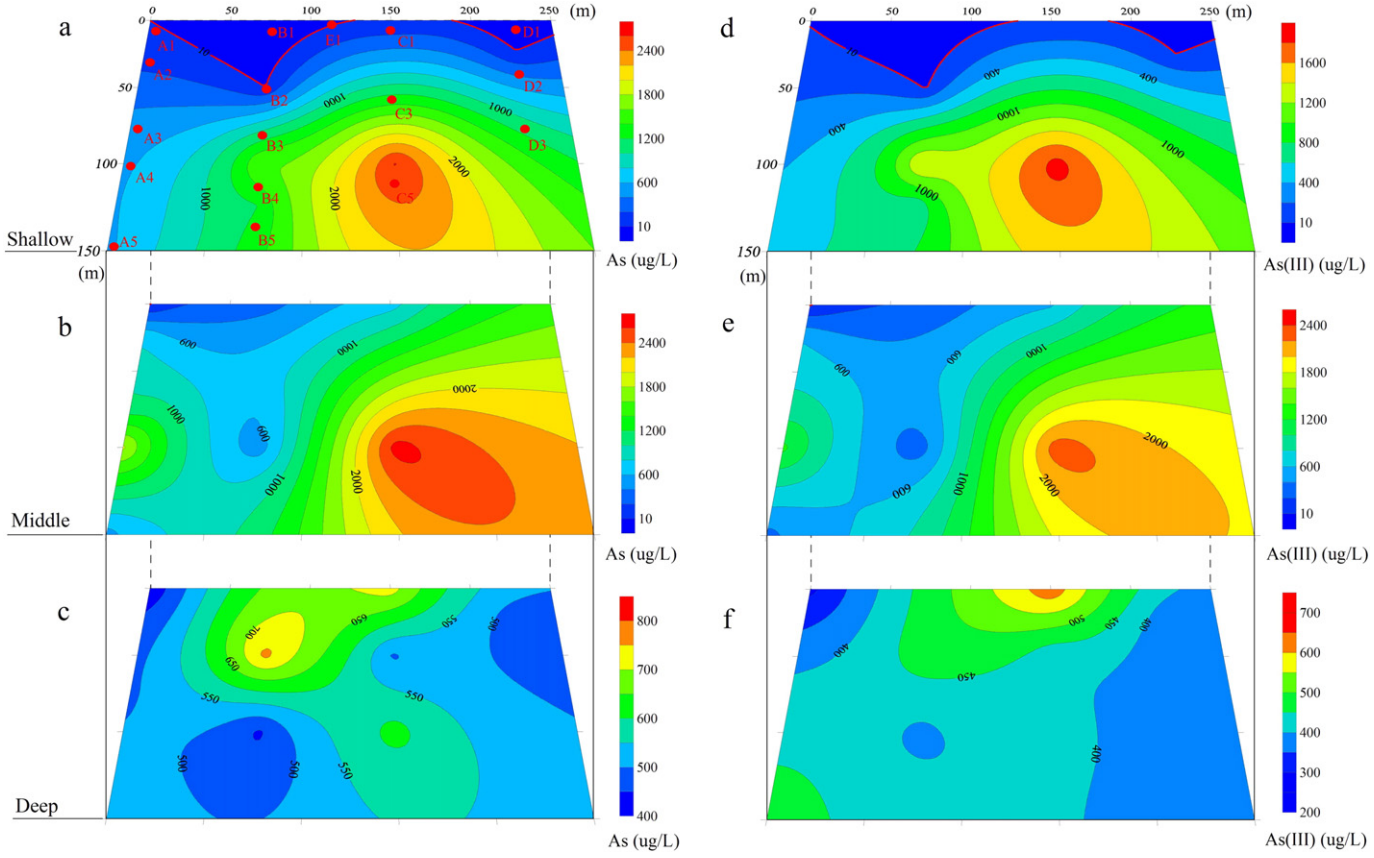

Fig. 3. Contour maps of groundwater As and As(III) concentration at the (a), (d) Shallow, (b), (e) Middle and (c), (f) Deep aquifer, respectively, with locations of the monitoring wells (labeled red solid circles) shown in (a).

mainly occurred in groundwater with pH values above 7.95, suggesting that the alkaline condition favors As enrichment in groundwater. The combination of high As with elevated Fe(II), HS^- and HCO_3^- concentration is likely indicative of the effects of microbially mediated Fe(III) and sulfate reduction on As mobilization in the presence of natural organic matter, since electron acceptors Fe(III) and SO_4^{2-} can be utilized by indigenous microorganisms to oxidize organic carbon, releasing Fe(II) and initially bound As, as well as HS^- and HCO_3^- into groundwater (Xie et al., 2013b). However, poor bivariate correlations ($\alpha = 0.05$ for all) of As with pH ($r^2 < 0.01$), Eh ($r^2 = 0.03$) and other redox-sensitive components (SO_4^{2-}, $r^2 = 0.10$; Mn, $r^2 = 0.08$; HS^-, $r^2 = 0.06$; NH_4^+, $r^2 < 0.01$, DOC, $r^2 < 0.01$; Fe^{2+}, $r^2 = 0.29$) imply that As mobilization is most probably constrained by multiple (bio)geochemical processes, involving pH-dependent adsorption, reductive dissolution of Fe(III) minerals, microbial reduction of SO_4^{2-} and biogenic formation of Fe(II) sulfide minerals with variable availability of labile organic carbon (Mukherjee et al., 2009). Moreover, As(V) and As(III) species were recognized to exhibit different geochemical behaviors during mobilization processes, with the neutral As(III) species more mobile under weakly alkaline and reducing conditions (Postma et al., 2007). It was also considered that distribution of solid-phase As in different pools exerted influences on As mobilization and its fate in aquifers, which needs further investigation on sediment geochemistry to reveal the transformation of As species between solid and aqueous phases (Xie et al., 2013a).

4.3. Sediment geochemistry

Geochemical analysis on sediment samples was conducted to understand potential effects of the form in which As is bound to solid-phase Fe minerals on As mobilization. Total solid-phase As in bulk sediments varied from 2.06 to 61.52 mg/kg, with a mean value of 27.73 mg/kg (Fig. 4),

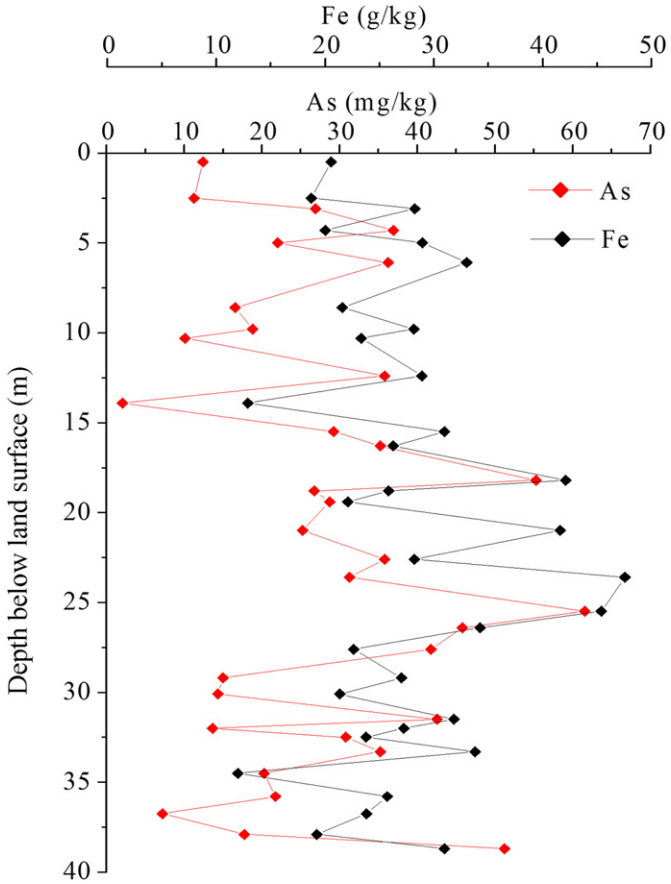

Fig. 4. Depth profiles of total As and Fe content in bulk sediments.

much higher than the average value of 5–10 mg/kg in modern unconsolidated sediments (Smedley and Kinniburgh, 2002). Such high contents of solid-phase As essentially provided direct source for aqueous As. It is noted that total Fe and As contents in sediments showed similar distribution patterns (Fig. 4) and a positive correlation can be discerned between them ($r^2 = 0.40$, $\alpha = 0.05$), indicating that Fe-bearing minerals may function as important sinks for As in aquifers, consistent with the view that solid-phase As was mostly bound to Fe oxide/hydroxides via strong adsorption and/or co-precipitation (Kneebone et al., 2002). However, despite high levels of As in sediments, both low and extremely high As concentration in groundwater infers that more than its source, mechanisms of As mobilization are significantly critical for its enrichment in groundwater.

Sequential extraction experiment was performed to understand the role of different solid-phase As speciation during As mobilization process. The sum of extractable As in the four fractions accounted for 41.30% to 88.62% of total solid-phase As (Table 2). The amount of $MgCl_2$-extractable As and As(III) was generally low, averaging at 0.71 and 0.03 mg/kg, respectively. Notably, most of ionically exchangeable As could be mobilized due to the increased ionic strength of groundwater with the presence of high concentration of Na^+ and HCO_3^-. The NaH_2PO_4-extractable As ranged from 1.37 to 34.89 mg/kg and accounted for 13.82% to 39.77% of total solid-phase As, indicating that chemical adsorption of As on mineral surfaces (mainly on metal oxides/hydroxides in the form of inner-sphere complexes) may be an important mechanism for As retention in sediments (Giménez et al., 2007). Solid-phase As in this pool was dominated by As(V) species, confirming As(V) can bind strongly to host minerals (Dixit and Hering, 2003; Giménez et al., 2007). The small amount of As(III) (av. 0.04 mg/kg) in this pool may be owing to some As(III) adsorption onto Fe and clay minerals under weakly alkaline conditions (Yang et al., 2005).

It is noted that As content in easily reducible Fe phase ranged from 1.37 to 38.25 mg/kg and mostly existed as As(V). Easily-reducible Fe content (normally in amorphous or poorly crystalline form) was also high, ranging from 3.71 to 10.27 g/kg and making up 16.52% to 31.99% of total Fe in sediments. Amorphous or poorly crystalline Fe oxides/hydroxides, widely present in aquifers, have remarkable affinity for negatively-charged As(V) owing to their high specific surface area and thus determine the availability of As in groundwater. High As content both in the NaH_2PO_4-extractable and easily reducible Fe-bound fractions demonstrates that As primarily binds to poorly crystalline Fe oxides/hydroxides via adsorption on the surfaces and/or co-precipitation during early deposition process (Giménez et al., 2007). This is also verified by the positive correlation ($r^2 = 0.74$, $\alpha = 0.05$) (Fig. 5a) between extractable Fe and As content in these two pools. As discussed above, elevated As concentration in groundwater was associated with high Fe(II) concentration under reducing conditions (Eh ≤ 100 mV). Therefore, reductive dissolution of and As desorption from Fe(III) oxides/hydroxides can control As enrichment in groundwater (Nickson et al., 2000; Postma et al., 2007).

The content of HCl-extractable As was lower than that in easily reducible Fe phase, varying from 0.97 to 12.47 mg/kg with an average of 2.72 mg/kg. Presumably, As in this pool was likely constrained in crystalline Fe minerals and secondary Fe(II) minerals (Borch et al., 2010; Xie et al., 2013a). It is interesting to note that significant amount of As(III) (up to 1.02 mg/kg, Table 2) was detected in this pool and Fe(II) equally accounted for a large part of the crystalline Fe (15.17% to 30.81%). Moreover, there was a good linear correlation ($r^2 = 0.77$, $\alpha = 0.05$) (Fig. 5b) between HCl-extractable As(III) and Fe(II) content, suggesting that As(III) in this pool may mainly co-exist with secondary Fe(II) minerals, such as $FeCO_3$ and Fe(II) sulfides (Kirk et al., 2004). Under sulfidic environment, as indicated by high sulfide concentration in groundwater, As may adsorb onto amorphous FeS, co-precipitate with authigenic mackinawite and pyrite or form As(III) sulfide minerals (Bostick et al., 2004; Jacks et al., 2013).

Table 2
Summary of As and Fe contents in sediments from the sequential extraction procedures.

	MG		PHOS		NH				HCl				TOT		As–S/As–T[a] (%)	Fe(II)–H/Fe–H[b] (%)
	As(III)	As	As(III)	As	As(III)	As	Fe(II)	Fe	As(III)	As	Fe(II)	Fe	As	Fe		
Max.	0.15	4.20	0.56	34.89	0.12	38.25	10.26	10.27	1.02	12.47	3.84	25.31	132.8	51.57	88.62	30.81
Min.	n.d.	0.24	n.d.	1.37	0.01	1.37	3.63	3.71	0.02	0.97	0.54	3.03	5.97	14.35	41.30	15.17
Aver.	0.03	0.71	0.04	6.06	0.01	5.58	5.51	5.66	0.19	2.72	1.45	6.93	26.20	24.46	61.08	21.91

Notes: Units: As, As(III): mg/kg, Fe, Fe(II): g/kg; MG, PHOS, NH, HCl: extracted with $MgCl_2$, NaH_2PO_4, $NH_2OH{\cdot}HCl$, HCl, respectively; TOT: total content in bulk sediments; Fe(II) and Fe were not detected in the $MgCl_2$ and NaH_2PO_4 extraction steps; n.d.: not detected.
[a] Percentage of sum of As from the four fractions in total As.
[b] Percentage of Fe(II) in total Fe from the HCl extraction step.

4.4. Geochemical processes controlling As transport

4.4.1. Desorption

Under weakly alkaline conditions, pH influence on the mobilization of As(V) and As(III) species can be different. The plot of $As(III)/As_{total}$ ratio versus pH value of groundwater samples exhibited two trends (Fig. 6). In trend 1, the $As(III)/As_{total}$ ratio was relatively low (<0.5) and decreased with pH increase from 7.69 to 8.04. From Fig. 7 it can be found that As mainly existed as $HAsO_4^{2-}$ bound to Fe oxides/hydroxides ($\equiv OHAsO_4^{3-}$) in moderately reducing zones (Eh ≥ 100 mV). However, the decrease in $As(III)/As_{total}$ ratio indicates that with pH increase, more As(V) was probably mobilized as a result of pH-dependent As(V) desorption from Fe oxides/hydroxides surfaces (Dixit and Hering, 2003). Our previous study also demonstrated that high As concentration in groundwater with pH increase from 7.2 to 8.8 was attributed to As desorption from Fe oxide surfaces (Xie et al., 2008). Modeling calculation based on diffuse double layer model for HFO also evidenced that As(V) species showed non-linear adsorption isotherm against pH value, and As(V) largely desorbed from Fe oxide surfaces with pH >7.5 (Smedley and Kinniburgh, 2002). In trend 2, high $As(III)/As_{total}$ ratio was nearly independent of pH variation. The neutral H_3AsO_3 became predominant in As species, and its desorption little relied on pH value of 8.04 to 8.34 (Dixit and Hering, 2003). Therefore, As(III) enrichment in groundwater may be primarily a result of As(V) reduction and As(III) mobilization from sediments due to its weak adsorption capacity under more reducing conditions (Eh ≤ 100 mV).

Studies proposed that major constitutes in natural waters, such as negatively charged HCO_3^-, SO_4^{2-}, and HPO_4^{2-} could drive As mobilization through competitive adsorption on the surface sites (Kanematsu et al., 2013; Radu et al., 2005; Zhao and Stanforth, 2001). Potential competitive anions in the study site were mainly HCO_3^- and SO_4^{2-}. However, no apparent correlation existed between concentration of groundwater As(V) and As(III) species and HCO_3^- (Fig. 8a–b). The concentration of As(V) and As(III) both firstly increased with that of HCO_3^- (approximately <450 mg/L), which seems to support that HCO_3^- outcompete As from Fe mineral surfaces. However, it is noted that lowest As was detected in those samples with higher HCO_3^- concentration. The reason may be that competitive effect of HCO_3^- was restrained by stronger chemical adsorption of As(V) on Fe minerals in the form of inner-sphere complexation, compared to non-specific electrostatic attraction of HCO_3^- to the surfaces (Sherman and Randall, 2003). Additionally, As(III) existed mainly as neutral species in groundwater, and its adsorption process is rarely affected by the negatively charged HCO_3^-. The concentration of As(V) and As(III) in groundwater generally increased with the decrease of sulfate (Fig. 8c–d). This can be explained by our finding that As mobilization was linked to the reduction of Fe(III), As(V) and sulfate coupled to the oxidation of organic matter in aquifers (Xie et al., 2013b). Microbial sulfate reduction produced aqueous sulfide that could reduce both As-bearing Fe oxides/hydroxides and As(V) species to increase As(V) and As(III) concentration in groundwater (Burton et al., 2011). Therefore, although HCO_3^- and SO_4^{2-} were considered to drive As desorption from Fe mineral surfaces, their relationships in this study indicate that redox reactions are more conspicuous in controlling As mobilization.

4.4.2. Sequential reduction

Under reducing conditions, Fe oxides/hydroxides in sediments can be reductively dissolved to produce aqueous Fe(II), leading to mobilization of bound As(V) into groundwater. However, scenarios for the Datong aquifers are more complex with regard to such a mechanism. It can be found As(V) concentration roughly increased with that of Fe(II), exhibiting a weak positive correlation (Fig. 9a, $r^2 = 0.31$, $\alpha = 0.05$). This may be the combined results of As pH-

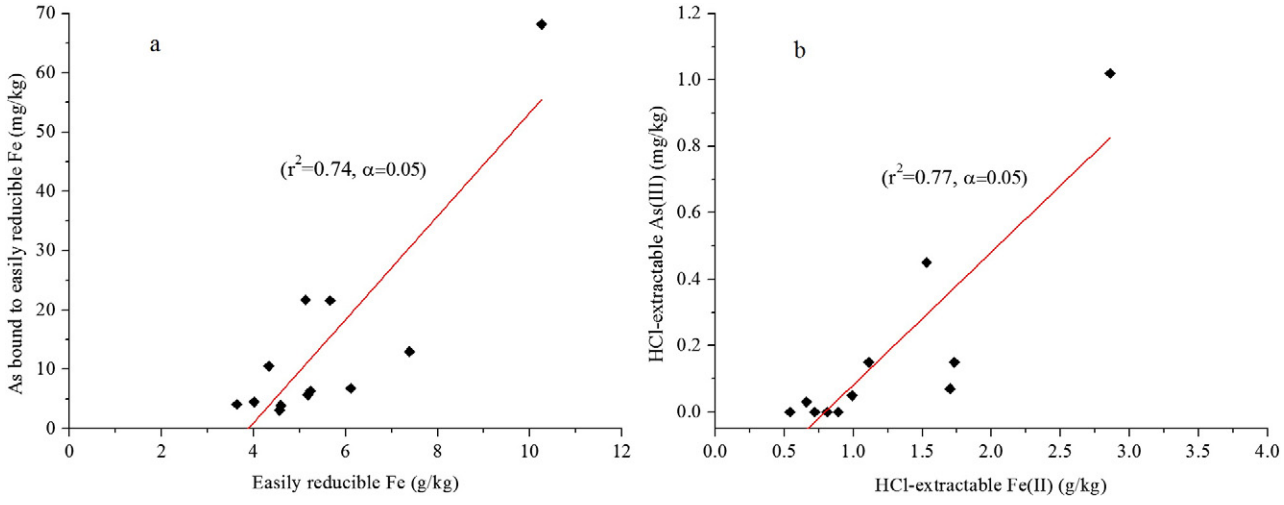

Fig. 5. Relationships between As and Fe content from (a) $NH_2OH{\cdot}HCl$ and (b) HCl extraction procedures. In (a), *NaH_2PO_4-extractable As* is included in *As bound to easily reducible Fe.*

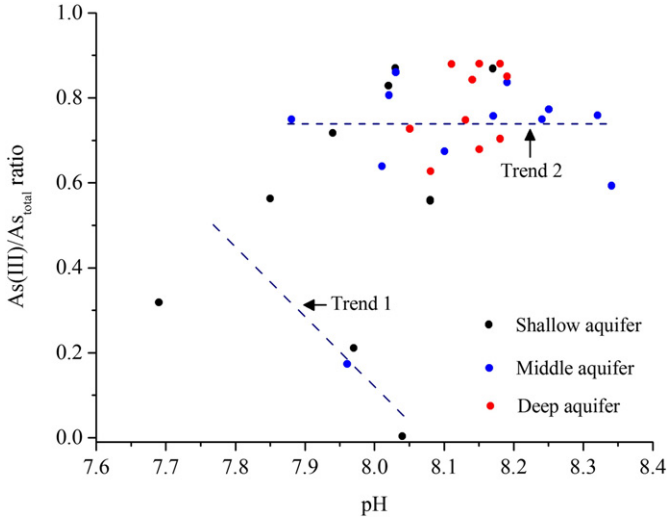

Fig. 6. Plot of As(III)/As$_{total}$ ratio versus pH value of groundwater samples from different aquifers.

dependent desorption and reductive dissolution of As-bearing Fe(III) oxides/hydroxides. Under moderately reducing conditions (Eh ≥ 100 mV), As(V) mobilization was mainly controlled by the desorption process, elevating As(V) concentration while aqueous Fe(II) concentration kept low (<0.05 mg/L). However, with the prevailing of more reducing environment, intensive reductive dissolution of Fe(III) oxides/hydroxides became dominated, releasing substantial As(V) and Fe(II) into groundwater. Another process contributing to this weak relationship could be the re-adsorption of As(V) onto Fe(III) oxides/hydroxides or secondary Fe(II) minerals to scavenge As(V) and Fe(II) from groundwater (Burnol and Charlet, 2010). This hypothesis can be inferred from the high content of As(V) in $MgCl_2$- and NaH_2PO_4-extractable As pools.

It is interesting to note that different from aqueous As(V) species, two obvious trends were observed in the relationship between As(III) versus Fe(II) concentration (Fig. 9b). Sequential redox reduction of Fe(III), As(V) and SO_4^{2-} can be responsible for those trends. In trend 1, As concentration showed a good linear relationship

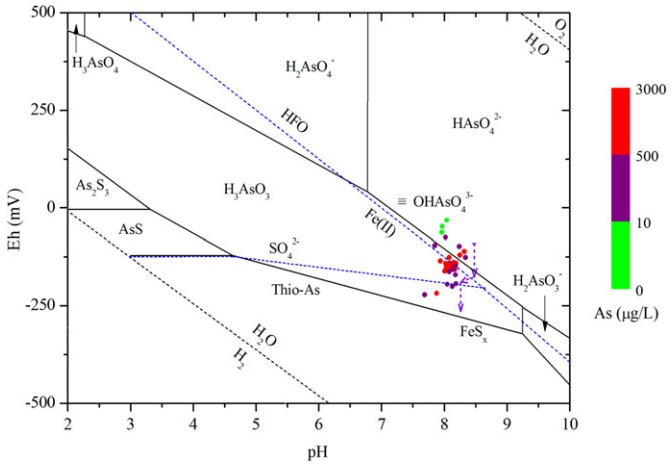

Fig. 7. Groundwater As distribution in the Eh-pH diagram for As–Fe–S system at 25 °C and 1 bar. The blue dash lines delineate the stability fields of Fe and S species. HFO: hydrous ferric oxides; $\equiv OHAsO_4^{3-}$: a $HAsO_4^{2-}$ sorption complex on HFO. The level of 500 μg/L is inserted to differentiate those extremely high As samples. The dash lines with arrows indicate the proposed As transport pathway.

($r^2 = 0.74$, $\alpha = 0.05$) with aqueous Fe(II), indicating that As(III) mobilization is simultaneously regulated by reductive dissolution of Fe(III) oxides/hydroxides and As(V) reduction reactions. High natural organic carbon (av. 9.39 mg/L) available in the anoxic aquifers served as an important energy source for microbial respiration and electron donor for the reduction of Fe(III) and As(V), and thus played a key role in As(III) enrichment in groundwater, as confirmed by observed depleted $\delta^{13}C$ value of dissolved inorganic carbon in high As groundwater during microbial mineralization of organic matters (Xie et al., 2013b). Accordingly, predominance of H_3AsO_3 (high As(III)/As$_{total}$ ratio in Fig. 6) within the stability field of Fe(II) (Fig. 7) imply that reduction of As(V) to As(III) probably coincided with reductive dissolution of Fe(III) oxides/hydroxides, resulting in simultaneous elevation of Fe(II) and As(III) in groundwater (Campbell et al., 2006; Herbel and Fendorf, 2006; Kocar and Fendorf, 2009). However in trend 2, As(III) concentration decreased to a moderate level (around 500 μg/L) and was independent of Fe(II) variation. Under strongly reducing conditions (Eh value down to −221.7 mV), subsequent sulfate reduction produced zero-valent sulfur and sulfide into groundwater, and reactions between As and the reduced S species became significant. High affinity of sulfur with As(V) can result in the complexation of S(−II) with As(V) to form thioarsenate and/or thioarsenite (both referred to as thioarsenic) and subsequent transformation into As(III) under alkaline conditions (Fisher et al., 2008; Planer-Friedrich and Wallschläger, 2009). Moreover, aqueous sulfide can also serve as an electron donor to microbially mediate As(V) reduction into As(III) under the sulfidic condition, a process enhancing As migration from Fe mineral surfaces (Burton et al., 2011; Fisher et al., 2008). These processes can take place in the absence of Fe(III) reduction and promote As(III) release into groundwater, thus contributing to the near irrelevance between As(III) and Fe(II) concentration within this trend. The control of sulfide on As(III) mobilization can be inferred from Fig. 7 where Eh values for stability fields of H_3AsO_3 and thioarsenic (referred to as Thio-As) were in line with measured Eh values of groundwater samples (Couture and Van Cappellen, 2011). It can also be found that groundwater samples falling around trend 2 mostly had elevated concentration of aqueous sulfide (Fig. 9d).

Those samples grouped around trend 2 contained lower As concentration than those around trend 1 (Fig. 9b). Aqueous Fe(II) was generally low in those samples with high sulfide concentration (Fig. 9c). Normally, dissolved sulfide and Fe(II) species derived from Fe(III) and SO_4^{2-} reduction can react to form insoluble Fe(II) sulfides, which preferentially occurs under reducing environments, to remove Fe(II) from groundwater (Jacks et al., 2013). Microbially mediated reduction of sulfate and subsequent formation of Fe(II) sulfide precipitates were also verified by Fe isotope evidence from our previous study at Datong Basin (Xie et al., 2013a). Results of geochemical modeling reveal that most of the groundwater samples were oversaturated with respect to mackinawite (FeS_m) (Fig. 10), a disordered Fe(II) sulfide mineral firstly to form in conditions representative of our study site and show strong affinity for As (Omoregie et al., 2013). Furthermore, As(V) and As(III) concentration both firstly increased with saturation indices (SI) of FeS_m, but then dramatically decreased to a low level (approximately <200 μg/L for As(V) and <500 μg/L for As(III) at SI > 1.0) (blue dashed ellipses in Fig. 10a–b). The reason for such a change may be that when continued sulfidization of Fe(II) under strongly reducing conditions (Eh ≤ 160 mV) reached the state of FeS_m precipitation, previously mobilized As would be sequestered by the newly-formed secondary mineral (via surface adsorption and/or co-precipitation), thereby decreasing As concentration in groundwater (Kirk et al., 2004; Saalfield and Bostick, 2009). This process is also verified by above results of sequential extraction with HCl and the inclusion of moderate-level As groundwater samples in the stability field of FeS_m (Fig. 7). Therefore, As re-immobilization to sediments under the sulfidic environment most likely interprets the decrease in As concentration in groundwater.

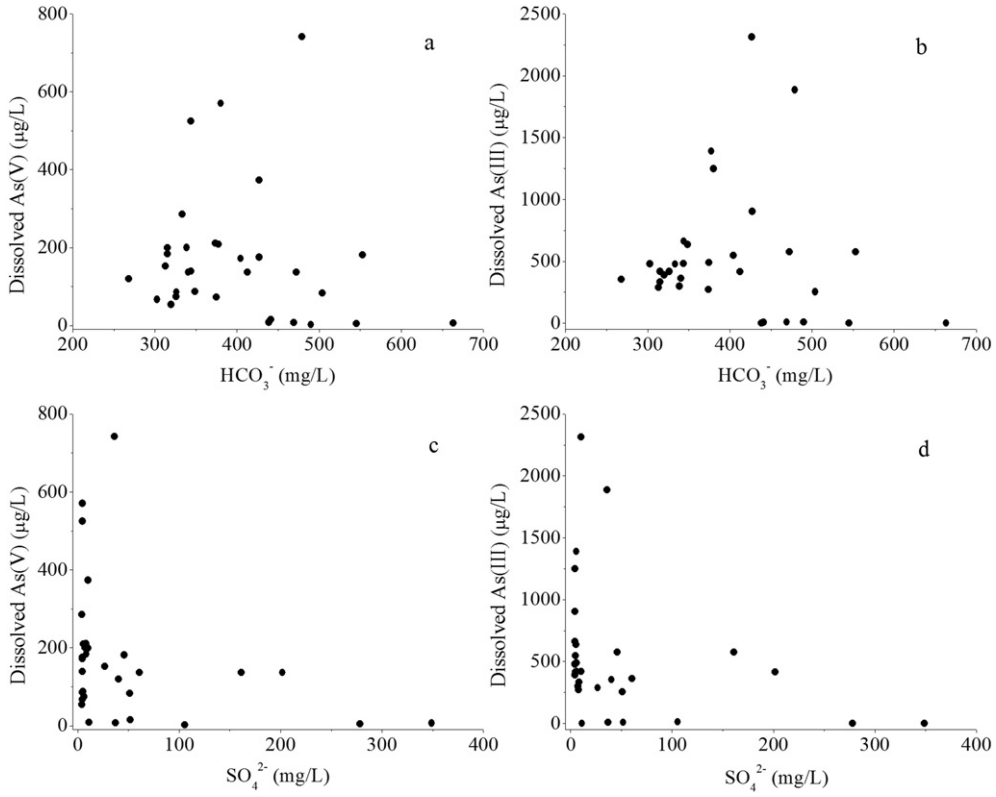

Fig. 8. Plots of As(III) or As(V) versus (a), (b) HCO_3^- and (c), (d) SO_4^{2-} concentration in groundwater.

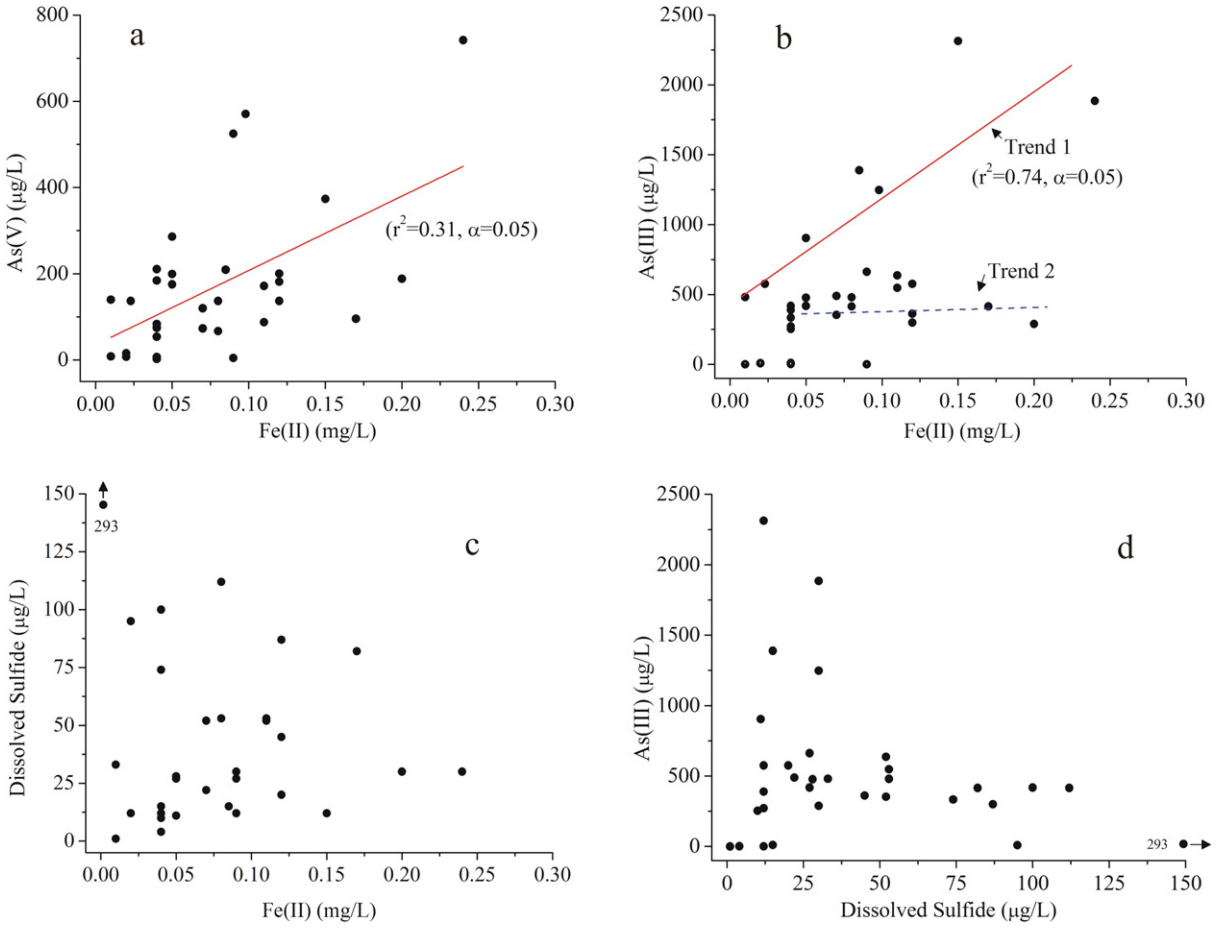

Fig. 9. Plots of (a) As(V), (b) As(III), (c) sulfide versus Fe(II) concentration and (d) As(III) versus dissolved sulfide in groundwater.

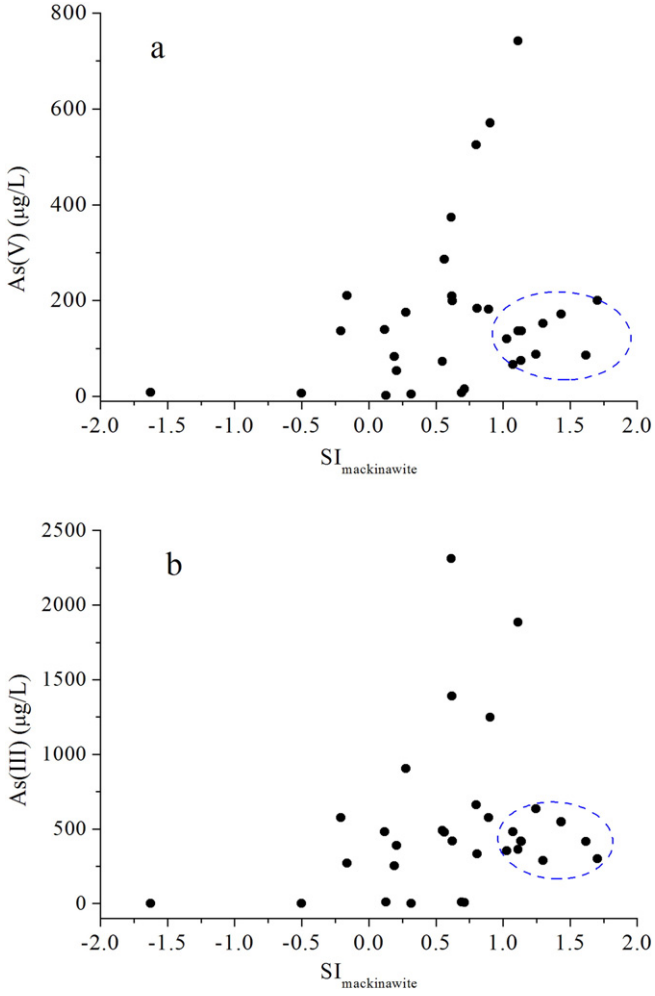

Fig. 10. Plots of (a) As(V) and (b) As(III) concentration versus saturation indices of mackinawite ($SI_{mackinawite}$) in groundwater.

4.4.3. Pathway of As transport

The above discussions have elaborated the effects of multiple geochemical processes, including desorption and sequential redox reactions, on the mobilization of different As species into groundwater. Studies conducted in other regions of the world, such as India, Bangladesh and Vietnam, also indicated that naturally occurring high-As groundwater was closely associated with alkaline and reducing conditions (Eiche et al., 2008; Polizzotto et al., 2005; Polya et al., 2005). The As migration from Fe minerals usually occurs with microbially mediated redox coupling of Fe(III), sulfate and natural organic carbon. To establish a generic model for As transport and enrichment in groundwater systems under common reducing, alkaline and sluggish groundwater conditions, the following As transport pathway is intentionally proposed (refer to the dashed line with arrow in Fig. 7): As primarily co-existed with Fe oxides/hydroxides via chemical adsorption and/or co-precipitation in sediments. Under groundwater conditions of pH value less than 7.69 and Eh higher than −100 mV, As mostly remained retarded on Fe oxides/hydroxides due to their strong affinity for As(V) species. This may explain why low As concentration was detected in some groundwater samples from the Shallow aquifer (Fig. 6). However, when the pH condition evolved to be weakly alkaline (pH > 7.69), significant As(V) release from Fe minerals surfaces was likely triggered by pH-dependent and competitive adsorption processes. With the prevalence of more reducing conditions (Eh ≤ 100 mV), reductive dissolution of Fe oxides/hydroxides and reductive desorption of As(V) jointly led to accumulation of both Fe(II) and As(III) in groundwater under sluggish flow zones. The As(III) species became predominant in the reducing aquifers. Under strongly reducing conditions (Eh ≤ 160 mV), zero-valent sulfur ($S^0_{(aq)}$) and sulfide (HS^-) produced from microbially mediated sulfate reduction may promote the transformation of As(V) into thioarsenic and further to As(III) without the involvement of Fe(III) reduction, as indicated by the independence of As(III) on Fe(II)variation and by the presence of high aqueous sulfide (Couture and Van Cappellen, 2011). On the other hand, dissolved sulfide also reacted with Fe(II) to form Fe(II) sulfide minerals. Some amounts of As(III) and As(V) can be re-adsorbed or co-precipitated into the minerals, thus decreasing As concentration in groundwater. These mechanisms shed new light into As enrichment and spatial distribution patterns in groundwater systems under hydrogeochemical conditions similar to Datong Basin.

5. Conclusions

Multilevel hydrogeochemical investigations in this study provide comprehensive recognition on the genesis of high-As groundwater in Datong Basin. Base on the observations toward a typical As-contaminated site at central part of this basin, the following can be concluded:

(1) As concentration in groundwater was highly spatially variable from 5.47 to 2690 μg/L, and high-As groundwater was characterized by high percentages of As(III) species (av. 67.9% of As_{total}), elevated Fe(II), HS^-, and NH_4^+ concentration and low redox potential.
(2) High As content was detected in aquifer sediments with an average of 27.73 mg/kg. The sequential extraction results demonstrate large amounts of As was mainly bound to poorly crystalline Fe oxides/hydroxides probably via strong adsorption and/or co-precipitation.
(3) Under reducing conditions (Eh ≤ 100 mV), extensive As migration was controlled by reductive dissolution of As-bearing Fe oxides/hydroxides and concurrent reductive desorption of As(V). In addition, sulfate reduction may cause As(V) transformation into thioarsenate and/or thioarsenite, promoting the enrichment of As(III) in groundwater. However, As(V) mobilization was mainly controlled by pH-dependent desorption under moderately reducing environment (Eh ≥ 100 mV).
(4) Significant decrease in As concentration with increased saturation indices of mackinawite suggests some amounts of As could have been re-sequestered by secondary Fe(II)-sulfide precipitates.

Acknowledgments

The authors would like to thank the anonymous reviewers for their constructive suggestions and comments on this manuscript. The research work was financially supported by the National Natural Science Foundation of China (No. 41120124003), the Ministry of Science and Technology of China (2012AA062602), the Ministry of Education of China (111 Project and Priority Development Projects of SRFDP (20120145130001)) and the Center of Hydrogeology and Environmental Survey, China Geological Survey (12120113103700).

References

Borch, T., Kretzschmar, R., Kappler, A., Van Cappellen, P., Ginder-Vogel, M., Voegelin, A., Campbell, K., 2010. Biogeochemical redox processes and their impact on contaminant dynamics. Environ. Sci. Technol. 44, 15–23.
Bose, P., Sharma, A., 2002. Role of iron in controlling speciation and mobilization of arsenic in subsurface environment. Water Res. 36, 4916–4926.
Bostick, B.C., Chen, C., Fendorf, S., 2004. Arsenite retention mechanisms within estuarine sediments of Pescadero, CA. Environ. Sci. Technol. 38, 3299–3304.

Burnol, A., Charlet, L., 2010. Fe(II)-Fe(III)-bearing phases as a mineralogical control on the heterogeneity of arsenic in southeast Asian groundwater. Environ. Sci. Technol. 44, 7541–7547.
Burton, E.D., Johnston, S.G., Bush, R.T., 2011. Microbial sulfidogenesis in ferrihydrite-rich environments: effects on iron mineralogy and arsenic mobility. Geochim. Cosmochim. Acta 75, 3072–3087.
Burton, E.D., Johnston, S.G., Planer-Friedrich, B., 2013. Coupling of arsenic mobility to sulfur transformations during microbial sulfate reduction in the presence and absence of humic acid. Chem. Geol. 343, 12–24.
Campbell, K.M., Malasarn, D., Saltikov, C.W., Newman, D.K., Hering, J.G., 2006. Simultaneous microbial reduction of iron(III) and arsenic(V) in suspensions of hydrous ferric oxide. Environ. Sci. Technol. 40, 5950–5955.
Charlet, L., Chakraborty, S., Appelo, C.A.J., Roman-Ross, G., Nath, B., Ansari, A.A., Lanson, M., Chatterjee, D., Mallik, S.B., 2007. Chemodynamics of an arsenic "hotspot" in a West Bengal aquifer: a field and reactive transport modeling study. Appl. Geochem. 22, 1273–1292.
Couture, R.-M., Van Cappellen, P., 2011. Reassessing the role of sulfur geochemistry on arsenic speciation in reducing environments. J. Hazard. Mater. 189, 647–652.
Dixit, S., Hering, J.G., 2003. Comparison of arsenic(V) and arsenic(III) sorption onto iron oxide minerals: Implications for arsenic mobility. Environ. Sci. Technol. 37, 4182–4189.
Eiche, E., Neumann, T., Berg, M., Weinman, B., van Geen, A., Norra, S., Berner, Z., Trang, P.T.K., Viet, P.H., Stüben, D., 2008. Geochemical processes underlying a sharp contrast in groundwater arsenic concentrations in a village on the Red River delta, Vietnam. Appl. Geochem. 23, 3143–3154.
Fendorf, S., Michael, H.A., van Geen, A., 2010. Spatial and temporal variations of groundwater arsenic in south and southeast Asia. Science 328, 1123–1127.
Fisher, J.C., Wallschlager, D., Planer-Friedrich, B., Hollibaugh, J.T., 2008. A new role for sulfur in arsenic cycling. Environ. Sci. Technol. 42, 81–85.
Freikowski, D., Neidhardt, H., Winter, J., Berner, Z., Gallert, C., 2013. Effect of carbon sources and of sulfate on microbial arsenic mobilization in sediments of West Bengal, India. Ecotoxicol. Environ. Saf. 91, 139–146.
Giménez, J., Martínez, M., de Pablo, J., Rovira, M., Duro, L., 2007. Arsenic sorption onto natural hematite, magnetite, and goethite. J. Hazard. Mater. 141, 575–580.
Guo, H.M., Wang, Y.X., Shpeizer, G.M., Yan, S.L., 2003. Natural occurrence of arsenic in shallow groundwater, Shanyin, Datong Basin, China. J. Environ. Sci. Health A Tox. Hazard. Subst. Environ. Eng. 38, 2565–2580.
Höhn, R., Isenbeck-Schröter, M., Kent, D., Davis, J., Jakobsen, R., Jann, S., Niedan, V., Scholz, C., Stadler, S., Tretner, A., 2006. Tracer test with As (V) under variable redox conditions controlling arsenic transport in the presence of elevated ferrous iron concentrations. J. Contam. Hydrol. 88, 36–54.
Herbel, M., Fendorf, S., 2006. Biogeochemical processes controlling the speciation and transport of arsenic within iron coated sands. Chem. Geol. 228, 16–32.
Jacks, G., Šlejkovec, Z., Mörth, M., Bhattacharya, P., 2013. Redox-cycling of arsenic along the water pathways in sulfidic metasediment areas in northern Sweden. Appl. Geochem. 35, 35–43.
Jiang, J., Bauer, I., Paul, A., Kappler, A., 2009. Arsenic redox changes by microbially and chemically formed semiquinone radicals and hydroquinones in a humic substance model quinone. Environ. Sci. Technol. 43, 3639–3645.
Kanematsu, M., Young, T.M., Fukushi, K., Green, P.G., Darby, J.L., 2013. Arsenic (III, V) adsorption on a goethite-based adsorbent in the presence of major co-existing ions: modeling competitive adsorption consistent with spectroscopic and molecular evidence. Geochim. Cosmochim. Acta 106, 404–428.
Keon, N.E., Swartz, C.H., Brabander, D.J., Harvey, C.F., Hemond, H.F., 2001. Validation of an arsenic sequential extraction method for evaluating mobility in sediments. Environ. Sci. Technol. 35, 2778–2784.
Kirk, M.F., Holm, T.R., Park, J., Jin, Q., Sanford, R.A., Fouke, B.W., Bethke, C.M., 2004. Bacterial sulfate reduction limits natural arsenic contamination in groundwater. Geology 32, 953–956.
Kneebone, P.E., O'Day, P.A., Jones, N., Hering, J.G., 2002. Deposition and fate of arsenic in iron- and arsenic-enriched reservoir sediments. Environ. Sci. Technol. 36, 381–386.
Kocar, B.D., Fendorf, S., 2009. Thermodynamic constraints on reductive reactions influencing the biogeochemistry of arsenic in soils and sediments. Environ. Sci. Technol. 43, 4871–4877.
Le, X.C., Yalcin, S., Ma, M.S., 2000. Speciation of submicrogram per liter levels of arsenic in water: on-site species separation integrated with sample collection. Environ. Sci. Technol. 34, 2342–2347.
Manning, B.A., Goldberg, S., 1997. Adsorption and stability of arsenic(III) at the clay mineral–water interface. Environ. Sci. Technol. 31, 2005–2011.
Mukherjee, A., Bhattacharya, P., Shi, F., Fryar, A.E., Mukherjee, A.B., Xie, Z.M., Jacks, G., Bundschuh, J., 2009. Chemical evolution in the high arsenic groundwater of the Huhhot basin (Inner Mongolia, PR China) and its difference from the western Bengal basin (India). Appl. Geochem. 24, 1835–1851.
Nickson, R.T., McArthur, J.M., Ravenscroft, P., Burgess, W.G., Ahmed, K.M., 2000. Mechanism of arsenic release to groundwater, Bangladesh and West Bengal. Appl. Geochem. 15, 403–413.
Omoregie, E.O., Couture, R.-M., Van Cappellen, P., Corkhill, C.L., Charnock, J.M., Polya, D.A., Vaughan, D., Vanbroekhoven, K., Lloyd, J.R., 2013. Arsenic bioremediation by biogenic iron oxides and sulfides. Appl. Environ. Microbiol. 79, 4325–4335.
Pedersen, H.D., Postma, D., Jakobsen, R., 2006. Release of arsenic associated with the reduction and transformation of iron oxides. Geochim. Cosmochim. Acta 70, 4116–4129.
Planer-Friedrich, B., Wallschläger, D., 2009. A critical investigation of hydride generation-based arsenic speciation in sulfidic waters. Environ. Sci. Technol. 43, 5007–5013.
Polizzotto, M.L., Harvey, C.F., Sutton, S.R., Fendorf, S., 2005. Processes conducive to the release and transport of arsenic into aquifers of Bangladesh. Proc. Natl. Acad. Sci. U. S. A. 102, 18819–18823.
Polya, D.A., Gault, A.G., Diebe, N., Feldman, P., Rosenboom, J.W., Gilligan, E., Fredericks, D., Milton, A.H., Sampson, M., Rowland, H.A.L., Lythgoe, P.R., Jones, J.C., Middleton, C., Cooke, D.A., 2005. Arsenic hazard in shallow Cambodian groundwaters. Mineral. Mag. 69, 807–823.
Postma, D., Larsen, F., Hue, N.T.M., Duc, M.T., Viet, P.H., Nhan, P.Q., Jessen, S., 2007. Arsenic in groundwater of the Red River floodplain, Vietnam: controlling geochemical processes and reactive transport modeling. Geochim. Cosmochim. Acta 71, 5054–5071.
Radu, T., Subacz, J.L., Phillippi, J.M., Barnett, M.O., 2005. Effects of dissolved carbonate on arsenic adsorption and mobility. Environ. Sci. Technol. 39, 7875–7882.
Roman-Ross, G., Cuello, G.J., Turrillas, X., Fernandez-MArtinez, A., Charlet, L., 2006. Arsenite sorption and coprecipitation with calcite. Chem. Geol. 233, 328–336.
Saalfield, S.L., Bostick, B.C., 2009. Changes in iron, sulfur, and arsenic speciation associated with bacterial sulfate reduction in ferrihydrite-rich systems. Environ. Sci. Technol. 43, 8787–8793.
Sherman, D.M., Randall, S.R., 2003. Surface complexation of arsenie(V) to iron(III) (hydr)oxides: structural mechanism from ab initio molecular geometries and EXAFS spectroscopy. Geochim. Cosmochim. Acta 67, 4223–4230.
Smedley, P.L., Kinniburgh, D.G., 2002. A review of the source, behaviour and distribution of arsenic in natural waters. Appl. Geochem. 17, 517–568.
Stüben, D., Berner, Z., Chandrasekharam, D., Karmakar, J., 2003. Arsenic enrichment in groundwater of West Bengal, India: geochemical evidence for mobilization of As under reducing conditions. Appl. Geochem. 18, 1417–1434.
Sugár, É., Tatár, E., Záray, G., Mihucz, V.G., 2013. Field separation-based speciation analysis of inorganic arsenic in public well water in Hungary. Microchem. J. 107, 131–135.
Wang, Y., Shvartsev, S.L., Su, C., 2009. Genesis of arsenic/fluoride-enriched soda water: a case study at Datong, northern China. Appl. Geochem. 24, 641–649.
WHO, 2001. WHO environmental health criteria 224. Arsenic and arsenic compounds. World Health Organization, Geneva, Switzerland.
Xie, X., Ellis, A., Wang, Y., Xie, Z., Duan, M., Su, C., 2009. Geochemistry of redox-sensitive elements and sulfur isotopes in the high arsenic groundwater system of Datong Basin, China. Sci. Total Environ. 407, 3823–3835.
Xie, X., Johnson, T.M., Wang, Y., Lundstrom, C.C., Ellis, A., Wang, X., Duan, M., 2013a. Mobilization of arsenic in aquifers from the Datong Basin, China: evidence from geochemical and iron isotopic data. Chemosphere 90, 1878–1884.
Xie, X., Wang, Y., Ellis, A., Li, J., Su, C., Duan, M., 2013b. Multiple isotope (O, S and C) approach elucidates the enrichment of arsenic in the groundwater from the Datong Basin, northern China. J. Hydrol. 498, 103–112.
Xie, X., Wang, Y., Su, C., Liu, H., Duan, M., Xie, Z., 2008. Arsenic mobilization in shallow aquifers of Datong Basin: hydrochemical and mineralogical evidences. J. Geochem. Explor. 98, 107–115.
Yang, J.K., Barnett, M.O., Zhuang, J.L., Fendorf, S.E., Jardine, P.M., 2005. Adsorption, oxidation, and bioaccessibility of As(III) in soils. Environ. Sci. Technol. 39, 7102–7110.
Zhao, H.S., Stanforth, R., 2001. Competitive adsorption of phosphate and arsenate on goethite. Environ. Sci. Technol. 35, 4753–4757.